Silicagel support mediated nonphotolytic cleavage of the rhenium–rhenium bond of [{NC$_5$H$_4$N=NC$_6$H$_4$(R)}(CO)$_3$Re^0]$_2$. Synthesis of the monomeric species Re^I{NC$_5$H$_4$N=NC$_6$H$_4$(R)}(CO)$_3$Cl, crystal structure, spectroscopic and electron-transfer properties

R. Samanta [a], P. Munshi [a], B.K. Santra [a], N.K. Lokanath [b], M.A. Sridhar [b], J.S. Prasad [b], G.K. Lahiri [a],*

[a] *Department of Chemistry, Indian Institute of Technology, Bombay, Powai, Mumbai-400076, India*
[b] *Department of Physics, University of Mysore, Mysore-670006, India*

Abstract

The reaction of Re$_2$(CO)$_{10}$ with the 2-arylazopyridine ligand, L [L=NC$_5$H$_4$–N=N–C$_6$H$_4$(R), R=H, *o*-Me/Cl, *m*-Me/Cl] in dry THF under a dinitrogen atmosphere afforded a metal–metal bonded product of the type (L)(CO)$_3$Re^0–Re^0 (CO)$_3$(L) **1**. On a silica gel column and in the presence of chlorinated solvents (CHCl$_3$ or CH$_2$Cl$_2$) the complex **1** transformed into a mononuclear complex of composition Re^I(L)(CO)$_3$Cl **2**, where the cleavage of Re–Re bond of **1** and the oxidative addition of chlorine to the rhenium center have taken place consecutively. The molecular structure of the complex **2a** (R=H) has been determined by single crystal X-ray diffraction. The crystal lattice consists of two crystallographically independent Re(L^1)(CO)$_3$Cl molecules which are non-superimposable mirror images; d and l enantiomers, exist in a 1:1 ratio. The complexes **2** display irreversible Re^I→Re^{II} oxidation processes near 1.5 V versus SCE and two quasi-reversible azo (N=N) reductions in the ranges −0.28 to −0.48 V and −0.83 to −1.06 V versus SCE. The complexes of the type **1** exhibit only four successive azo reductions in the range 0 to −2 V versus SCE. Both the complexes (**1** and **2**) display dπ(Re)→π*L metal-to-ligand charge-transfer transitions near 500 nm and intraligand n–π* and π–π* transitions near 400 and 300 nm, respectively. The complexes **2** are susceptible to a spontaneous chloride exchange reaction. © 1999 Elsevier Science S.A. All rights reserved.

Keywords: 2-Arylazopyridine; Rhenium; Cleavage of rhenium–rhenium bond; Electron transfer

1. Introduction

There has been continuous research activity on the reaction studies of dirhenium decacarbonyl, Re$_2$(CO)$_{10}$. This is primarily due to its photo- and thermal-induced versatile reactive nature in solution [1]. Although photo-initiated reactions of Re$_2$(CO)$_{10}$ proceed with a substantial degree of homolytic Re–Re bond scission, metal–metal bond homolysis is not the primary step for thermally initiated substitution of Re$_2$(CO)$_{10}$. Under strictly thermal conditions substitution proceeds by a dissociative pathway with CO loss, without any Re–Re bond breaking [2].

The present work originates from our interest in studying the reactivity pattern of Re$_2$(CO)$_{10}$ in the presence of the very strongly π-acidic unsymmetrical azoimine based arylazopyridine ligand [NC$_5$H$_4$N= NC$_6$H$_4$(R), L]. Under thermal conditions the interaction of Re$_2$(CO)$_{10}$ with the ligand L initially follows a substitution process with the loss of two CO molecules from each rhenium center affording a new

---

* Corresponding author. Fax: +91-22-578-3480.
E-mail address: lahiri@ether.chem.iitb.ernet.in (G.K. Lahiri)

class of stable metal–metal bonded product of the type $[(L)(CO)_3Re^0–Re^0(CO)_3(L)]$, **1**. However, on a silica gel column and in the presence of chlorinated solvent, $CHCl_3$ or CH_2Cl_2 the complex **1** unexpectedly transforms into a monomeric complex of the type $Re^I(L)(CO)_3Cl$ **2**. Here in the course of chromatography the cleavage of the rhenium–rhenium bond of **1** and the oxidative addition of a chlorine atom (generated by the cleavage of C–Cl bond of the chlorinated solvent) to the rhenium center have taken place consecutively on the silica gel support. To the best of our knowledge this work demonstrates the first example of a silica gel mediated rhenium–rhenium bond cleavage reaction followed by oxidative chlorine addition at the rhenium center.

Herein we report the synthetic account of the formation of complexes **1** and **2**, their spectroscopic properties, metal and ligand based electron-transfer properties and single crystal X-ray structure of a representative complex **2a**.

2. Results and discussion

2.1. Synthesis and characterization of the complexes

The five substituted arylazopyridine ligands (L) used for the present study are abbreviated as $L^1–L^5$. The reaction of $Re_2(CO)_{10}$ with the ligand L in freshly distilled dry tetrahydrofuran (THF) solvent under N_2 atmosphere results in a red–brown solution, from which the dark colored metal–metal bonded dimeric solid product of composition $\{(CO)_3 LRe^0–Re^0L(CO)_3\}$ **1** is isolated after removal of the solvent under reduced pressure (Scheme 1).

Although the complexes **1** are stable both in the solid and solution states, on the silica gel column and in the presence of chlorinated solvent, $CHCl_3$ or CH_2Cl_2 as eluent the red–brown colored complexes **1** have been transformed partially into a pink-colored complexes of composition $Re^I(L)(CO)_3Cl$ **2** (Scheme 1), leaving behind a dark band containing unchanged starting complexes **1** at the top of the column, which can be easily

eluted in the pure state by acetonitrile. The repetition of similar chromatographic operation on the unaltered complexes **1** (recovered from the previous column) result in a second batch of complexes **2** in the presence of $CHCl_3$ as eluent. Three or four repetitions of similar chromatographic cycles are required for the complete transformation of **1** to **2**.

Thus during the chromatographic process the metal–metal bond of complexes **1** have been cleaved and the oxidative chlorine addition (via the abstraction of chlorine atom from the chlorinated solvent, $CHCl_3$ or CH_2Cl_2) to the newly formed transient monomeric unit of **1** takes place.

Under dark conditions as well as in the presence of strong UV light the behavior of the complexes **1** with respect to the chromatographic operation does not alter at all as compared to normal laboratory light. Since the conversion of **1** to **2** does not occur alone in the chlorinated solvents ($CHCl_3$ or CH_2Cl_2) even under heating and the presence of laboratory light does not alter the rate of the conversion process from **1** to **2**, it can therefore be inferred that the silica gel support here plays an active role to cleave the Re–Re bond in **1** which leads eventually to the formation of the final product **2** in the presence of chlorinated solvent.

The reaction of **1** with the silica gel slurry in $CHCl_3$ or CH_2Cl_2 can also generate the complexes **2** but the rate of conversion ($1 \rightarrow 2$) is found to be much slower compared to the silica gel column.

Although the photolytic cleavage of the Re–Re bond of $Re_2(CO)_{10}$ and its derivatives is a well established process [2], the nonphotolytic silica gel mediated cleavage of the Re–Re bond of dirhenium complexes have been observed for the first time.

Microanalytical data (C, H, N) of **1** and **2** (Table 1) are in good agreement with the calculated values. The complexes (**1** and **2**) are nonconducting in acetonitrile solution and diamagnetic (Re^0, $t_{2g}^6 e_g^1$, the unpaired electron in the e_g level of each Re center gets paired up through the $Re^0–Re^0$ bond formation in **1**; Re^I in **2**, t_{2g}^6, $S = 0$).

2.2. Crystal structure of $Re^I(NC_5H_4N=NC_6H_5)(CO)_3Cl$ (2a)

The crystal structure of **2a** consists of two crystallographically independent $Re^I(NC_5H_4N=NC_6H_5)(CO)_3Cl$ molecules (**A** and **B**). A view of the molecules is shown in Fig. 1 and selected bond parameters are given in Table 2. Although the molecule possesses a pseudo C_2 axis, it is chiral since the mirror images are not superimposable. Thus the non-superimposable mirror images (**A** and **B**) are d and l enantiomers of the same optically active complex **2a**. Since in the crystal lattice the d and l enantiomers exist in a 1:1 ratio and since the molecule **2a** does not show any optical rotation in solution,

L^1	R = H	1a	2a
L^2	R = 8Me	1b	2b
L^3	R = 8Cl	1c	2c
L^4	R = 9Me	1d	2d
L^5	R = 9Cl	1e	2e
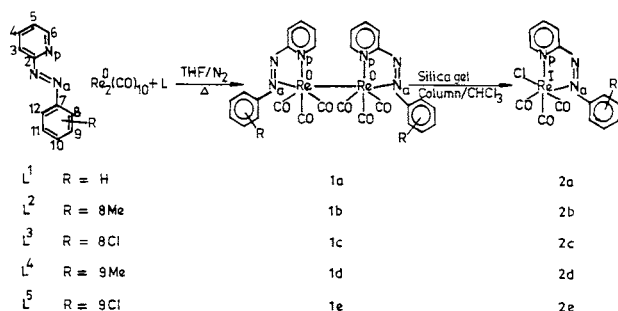
Scheme 1.

Table 1
Microanalytical, selected infrared and electronic spectral data

Compound	Elemental analysis (%)[a]			IR[b], ν_{max} (cm^{-1})			Electronic spectral data[c]
	C	H	N	CO	N=N	Re–Cl	λ_{max} (nm) (ε = dm^3 mol^{-1} cm^{-1})
1a	37.01 (37.07)	2.03 (1.99)	9.35 (9.27)	2027 1924 1884	1376	–	507(4079), 372(6996), 300(12140)
1b	38.62 (38.52)	2.41 (2.35)	(8.90) (8.98)	2041 1935 1920	1372	–	510(3695), 365(6500), 295(11100)
1c	34.53 (34.45)	1.67 (1.64)	8.53 (8.61)	2034 1936 1927	1375	–	514(4395), 378(7200), 305(12920)
1d	38.58 (38.52)	2.29 (2.35)	8.91 (8.98)	2034 1930 1905	1370	–	507(3342), 382(6375), 310(11772)
1e	34.54 (34.45)	1.60 (1.64)	8.69 (8.61)	2028 1925 1892	1370	–	517(4412), 381(7050), 298(12830)
2a	34.29 (34.37)	1.80 (1.84)	8.67 (8.59)	2022 1920 1881	1380	325	523(4660), 395(8940)[d], 337(11340)
2b	35.71 (35.80)	2.23 (2.18)	8.44 (8.35)	2038 1940 1910	1387	322	517(5090), 385(4700)[d], 304(8270)
2c	32.22 (32.11)	1.50 (1.53)	8.10 (8.03)	2038 1942 1920	1384	325	529(6670), 379(3620)[d], 304(10810)
2d	35.69 (35.80)	2.15 (2.18)	8.27 (8.35)	2030 1927 1890	1374	327	517(4570), 408(8320)[d], 381(10900)
2e	32.24 (32.11)	1.48 (1.53)	8.14 (8.03)	2032 1933 1886	1374	328	533(3730), 374(8720)[d], 318(17600)
3	33.64 (33.57)	2.27 (2.30)	9.14 (9.21)	2038 1938 1920	1382	–	447(6590), 404(6700), 336(7520)

[a] Calculated values are in parentheses.
[b] In KBr disk.
[c] In dichloromethane solution.
[d] Shoulder.

therefore the complex **2a** also represents the racemic mixture in the crystal. The bond distances and angles in the two molecules **A** and **B** are found to be slightly different (Table 2), which is presumably due to the effect of crystal packing forces.

The Re(N)$_2$(CO)$_3$Cl coordination sphere is distorted from regular octahedral geometry as can be seen from the angles subtended at the metal. The coordinated carbonyl groups are disposed facially. The five-mem-

bered chelate ring is planar. The acute chelate bite angles 72.4 (12)° and 71.1(11)° for **A** and **B** molecules, respectively are the major distorting factors in the structures. The dimensions of the chelate ring compare well with those found in the ruthenium [3], osmium [4] and other type of rhenium [5] chelates of L.

Reported Re^I–Cl distances lie in the range 2.49–2.52 Å [6]. The average Re–Cl length in the molecule **2a** [2.47(8) Å] is slightly shorter than the reported dis-

tances. The average Re–CO distance [1.87(4) Å] in **2a** is compared well with the reported Re^I–CO distances (1.85–1.88 Å) [6]. The average Re–N(pyridine), Re–N(azo) and N=N bond lengths in **2a** are, respectively 2.14(3), 2.15(5) and 1.25(5) Å, which fall within the limit of reported distances [5,7].

2.3. IR, UV-Vis, ^{1}H-NMR and FAB mass spectra

The complexes of both the type (**1** and **2**) exhibit similar IR spectra except in the metal halide region. Selected IR frequencies are listed in Table 1 and the carbonyl stretching frequencies are shown in Fig. 2. There are three notable features of the IR spectra: (i) Three distinct C≡O stretching vibrations in the range 2000–1850 cm^{-1} in each case. If the local symmetry of the complexes **2** is C_{3v}, two bands are expected with the irreducible representations A_1 and E. In the present cases, however, the doubly degenerated E vibrations are somewhat split, because the symmetry is lowered by the presence of unsymmetrical ligand L and Cl. A careful inspection of the carbonyl stretching frequencies of the dinuclear complexes **1** (Fig. 2(b)) indicate the presence of more than three bands possibly due to further reduction of symmetry in the complexes **1**. (ii) The azo stretching frequency of the coordinated ligand L is appreciably lowered (∼1380 cm^{-1}) compared to that in the free L (∼1425 cm^{-1}), evidently due to the d$_\pi$ Re→π*(L) back-bonding effect [8]. (iii) One sharp band near 325 cm^{-1} due to ν(Re–Cl) in each case of **2** has been observed, which is absent in the spectra of the complexes **1** as expected. A direct comparison of the IR spectra of complexes **1** and **2** reveal the presence of common (L)(CO)$_3$Re unit in both the complexes.

The Raman spectra of complexes **1** exhibit a band near 130 cm^{-1} corresponding to the Re–Re bond [9].

The complexes **1** and **2** display two major intense bands near 500 and 300 nm (Table 1). The higher energy band near 300 nm is associated with a shoulder at the lower energy part near 400 nm. The band near 500 nm is assigned to dπ(Re)→L(π*) (where L(π*) is believed to be dominated primarily by the LUMO of the azoimine chromophore [8]) MLCT transition. A transition of this type is well documented in low-spin rhenium (I) [10], ruthenium (II) [11], osmium (II) [12], cobalt(III) [13] complexes of unsaturated ligands.

The higher energy bands near 400 and 300 nm are presumably due to intra-ligand n–π* and π–π* transitions, respectively [14].

The complexes of both the type **1** and **2** exhibit similar ^{1}H-NMR spectra corresponding to one ligand L as the presence of mirror plane through the Re–Re bond in **1** makes each half of the molecule **1** equivalent. Spectral data for **2** are listed in Table 3. The pyridine proton signals appear in an isolated region except for the 5-H proton, and are clearly identified. The 8-H and 12-H protons appear as coincident doublets in complex **2a** whereas 8-H signal appears as a separate singlet for the *meta* substituted complexes **2d** and **2e**. Further, the 8-H singlet is significantly shifted to higher and lower fields in the complexes **2d** and **2e** respectively compared to **2a** (Table 3) based on the electron releasing and withdrawing properties of the methyl and chloride substituents, respectively. *Ortho* substituted complexes (**2b**
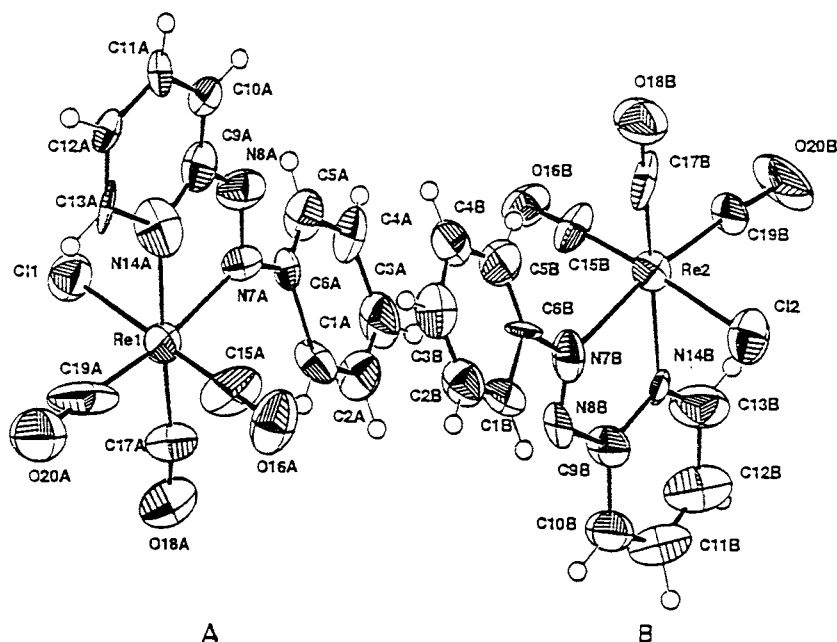

Fig. 1. Perspective view for two independent [Re^I(NC$_5$H$_4$N=NC$_6$H$_5$)(CO)$_3$Cl] molecules **2a**.

Table 2
Selected bond distances (Å) and angles (°) in **2a** (with estimated standard deviations in parentheses)

Distances

Re(1)–C(15A)	1.85(3)	Re(2)–C(15B)	1.90(3)
Re(1)–C(17A)	1.88(4)	Re(2)–C(17B)	1.88(3)
Re(1)–C(19A)	1.82(7)	Re(2)–C(19B)	1.96(4)
Re(1)–N(7A)	2.12(5)	Re(2)–N(7B)	2.19(5)
Re(1)–N(14A)	2.15(3)	Re(2)–N(14B)	2.13(3)
Re(1)–Cl(1)	2.452(8)	Re(2)–Cl(2)	2.499(7)
N(7A)–N(8A)	1.28(5)	N(7B)–N(8B)	1.19(5)

Angles

C(15A)–Re(1)–C(17A)	85.1(16)	C(17B)–Re(2)–C(15B)	93.3(11)
C(15A)–Re(1)–C(19A)	91(2)	C(19B)–Re(2)–C(15B)	87.4(19)
C(17A)–Re(1)–C(19A)	81(2)	C(17B)–Re(2)–C(19B)	90.8(17)
C(15A)–Re(1)–N(7A)	95.8(18)	C(15B)–Re(2)–N(7B)	92.4(17)
C(17A)–Re(1)–N(7A)	104.9(14)	C(17B)–Re(2)–N(7B)	101.0(15)
C(19A)–Re(1)–N(7A)	171.3(19)	C(19B)–Re(2)–N(7B)	168.2(15)
C(15A)–Re(1)–N(14A)	93.9(16)	C(15B)–Re(2)–N(14B)	94.5(10)
C(17A)–Re(1)–N(14A)	177.1(17)	C(17B)–Re(2)–N(14B)	169.1(14)
C(19A)–Re(1)–N(14A)	102(2)	C(19B)–Re(2)–N(14B)	97.2(13)
N(7A)–Re(1)–N(14A)	72.4(12)	N(14B)–Re(2)–N(7B)	71.1(11)
C(15A)–Re(1)–Cl(1)	178.9(16)	C(15B)–Re(2)–Cl(2)	176.0(17)
C(17A)–Re(1)–Cl(1)	95.9(10)	C(17B)–Re(2)–Cl(2)	89.0(9)
C(19A)–Re(1)–Cl(1)	89.9(16)	C(19B)–Re(2)–Cl(2)	95.9(13)
N(7A)–Re(1)–Cl(1)	83.5(7)	N(7B)–Re(2)–Cl(2)	83.9(7)
N(14A)–Re(1)–Cl(1)	85.1(9)	N(14B)–Re(2)–Cl(2)	82.9(6)

and **2c**) also exhibit the expected changes in the distribution of the phenyl ring proton signals with respect to the unsubstituted complex (**2a**). The chemical shift of the methyl group follows the order: *o*-Me (**2b**), 2.53 ppm > *m*-Me (**2d**), 2.37 ppm, indicating the effect of nearby electron withdrawing azo group on the *ortho* methyl group is more pronounced compared to the *meta* methyl group.

FAB mass spectra of the two representative complexes **1a** and **2a** were recorded. The molecular ion peaks are observed at m/z, 906.6 and 489 for **1a** and **2a,** respectively which are in good agreement with the calculated mass of the complexes **1a** (formula weight, 906.4) and **2a** (formula weight, 488.7), respectively.
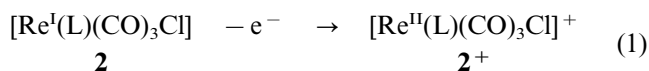
All our attempts to grow suitable single crystals for X-ray characterization of the complexes of type **1** have failed altogether. However, elemental analysis, conductivity, magnetic moment, FAB mass and spectral data collectively are in agreement with the composition and structure of **1**.

2.4. Electron-transfer properties

2.4.1. Metal redox

Electron-transfer properties of the complexes **1** and **2** have been studied by cyclic voltammetry in acetonitrile solvent using a platinum working electrode. The complexes **2** are electroactive with respect to the

metal as well as the ligand (L) centers and display the same three redox processes in the potential range ± 2 V versus SCE at 298 K, whereas the complexes **1** exhibit only the ligand reductions within the potential range ± 2 V versus SCE. Representative voltammograms are shown in Fig. 3 and the reduction potentials are listed in Table 4. Complexes **2** show one irreversible oxidation process, E_{pa} near 1.5 V versus SCE. The one-electron nature of this oxidation process is confirmed by direct comparison of its current height (i_{pa}) with that of the experimentally established one-electron reversible reduction process observed at the negative side of the SCE (see later) (Fig. 3). This oxidation process is assigned to the rhenium(I) to rhenium(II) oxidation, Eq. (1):

$$[\text{Re}^I(\text{L})(\text{CO})_3\text{Cl}] \quad -\text{e}^- \quad \rightarrow \quad [\text{Re}^{II}(\text{L})(\text{CO})_3\text{Cl}]^+ \tag{1}$$
$$\mathbf{2} \qquad\qquad\qquad\qquad\qquad \mathbf{2^+}$$

Since in the complexes **2** except for chloride all the other coordinated ligands (CO and L) are well-known strong π-acidic centers, therefore, the presence of strong π-acidic ligands around the metal ion in the coordination sphere stabilizes the Re^I state (t_{2g}^6 configuration) to a great extent and this is reflected in the high and irreversible Re^I → Re^{II} oxidation potential (ca. 1.5 V) [15]. The formal potential of Re(I) → Re(II) oxidation process (Eq. (1)) varies depending on the nature and the position of the substituents present in the ligand framework and it follows the order: **2d** < **2b** < **2a** < **2c** < **2e**.
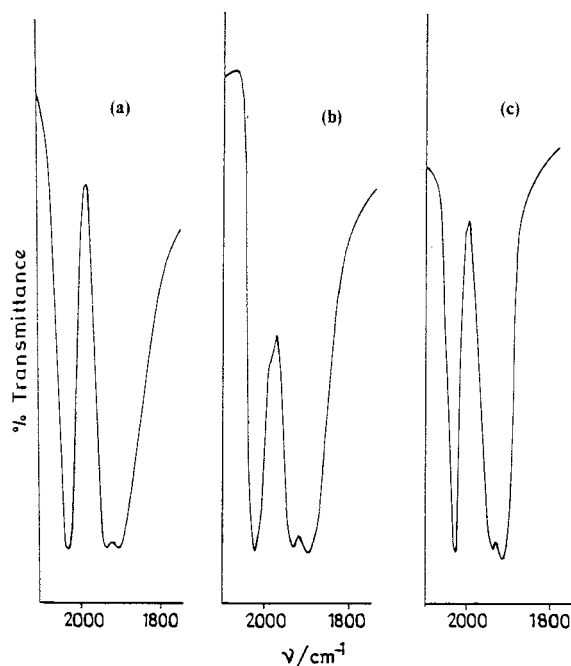

Fig. 2. Infrared spectra of (a) [Re^I{NC$_5$H$_4$N=NC$_6$H$_4$(*o*-Me)}(CO)$_3$Cl] **2b**; (b) [{NC$_5$H$_4$N=NC$_6$H$_4$(*o*-Me)}(CO)$_3$Re^0]$_2$ **1b**; (c) [Re^I{NC$_5$H$_4$N= NC$_6$H$_4$(*o*-Me)}(CO)$_3$(CH$_3$CN)]ClO$_4$ **3** in KBr disks.

Table 3
^{1}H-NMR spectral data in CDCl$_3$

δ (J)^a

Compound	H(6)	H(5)	H(4)	H(3)	H(8)	H(9)	H(10)	H(11)	H(12)
2a	9.04	7.68	8.26	8.61	7.99	7.60	7.64	7.60	7.99
	(5.5)^b	(6.2)^c	(7.4)^c	(7.9)^b	(7.2)^b	(7.1)^c	(6.2)^c	(7.1)^c	(7.2)^b
2b	9.04	7.71	8.27	8.59	Me	7.4^d	7.4^d	7.4^d	7.8
	(5.4)^b	(6.7)^c	(7.8)^c	(7.6)^b	2.53	–	–	–	(7.4)^b
2c	9.04	7.74	8.28	8.67	–	7.59	7.45	7.50	7.8
	(5.3)^b	(6.0)^c	(7.3)^c	(7.6)^b		(6.8)^b	(7.4)^c	(7.3)^c	(7.6)^b
2d	9.04	7.69	8.26	8.6	7.46^e	Me	7.48	7.67	7.82
	(5.3)^b	(6.6)^c	(8.0)^c	(7.6)^b		2.37	(7.7)^b	(7.0)^c	(7.5)^b
2e	9.05	7.71	8.28	8.64	8.04^e	–	7.98	7.45	7.93
	(5.5)^b	(6.9)^c	(8.3)^c	(7.8)^b			(7.51)^b	(6.8)^c	(7.6)^b

^{a} Tetramethylsilane is the internal standard.
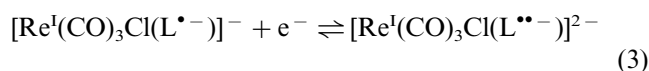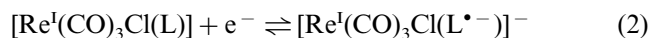^{b} Doublet.
^{c} Triplet.
^{d} Complex multiplet pattern centered at $\delta = 7.4$.
^{e} Singlet.

Under identical experimental conditions the complexes of type **1** on the other hand do not show any metal oxidation within $+2$ V versus SCE potential limit which indicates that under the metal–metal bonded dimeric environment as in **1** the rhenium ion gets preferentially stabilized in the zero oxidation state, which is certainly due to the perfect synchronization of the metal-oxidation state and the back-bonding effect under an environment of having only strong π-acidic ligands (CO and L) around the metal ion.

2.4.2. Ligand reduction

On the negative side of SCE two successive reversible reductions (the anodic and cathodic peak heights are equal and vary as the square root of the scan rate) are observed for all the complexes of type **2** (Fig. 3; Table 4). The observed two successive one-electron reductions for each of the complexes **2** are believed to be the reductions of azo group of the coordinated ligand L, Eqs. (2) and (3) [16].

$$[Re^I(CO)_3Cl(L)] + e^- \rightleftharpoons [Re^I(CO)_3Cl(L^{\bullet-})]^- \quad (2)$$

$$[Re^I(CO)_3Cl(L^{\bullet-})]^- + e^- \rightleftharpoons [Re^I(CO)_3Cl(L^{\bullet\bullet-})]^{2-} \quad (3)$$

The one-electron nature of the first reduction couple, Eq. (2) is confirmed by constant potential coulometry in acetonitrile solvent at 263 K. The coulometrically produced reduced brown solutions (**2**$^-$) (obtained by reducing the complexes **2** at a potential 100 mV negative to the corresponding E_{pc} of the first reduction couple (Fig. 3); n values: **2a**, 1.04; **2b**, 1.06; **2c**, 0.97; **2d**, 1.04; **2e**, 1.07; $n = Q/Q'$ where Q' is the calculated Coulomb count for a one-electron transfer and Q is that found after exhaustive electrolysis of 10^{-2} mmol

of solute) were unstable. However, we have succeeded in recording the EPR spectrum for the reduced complex **2b**$^-$ by quick freezing the electrolyzed solution (liquid nitrogen, 77 K). The reduced complex **2b**$^-$ displays an EPR signal with center field g value 2.0029. The hyperfine splittings due to nitrogen nuclear spin ($I = 1$) have been detected on both sides of the central intense line. This suggests that the unpaired electron in the reduced product **2**$^-$ is predominantly localized in a ligand character orbital [17]. Coulometric reduction of the second couple (Fig. 3) generated reduced species
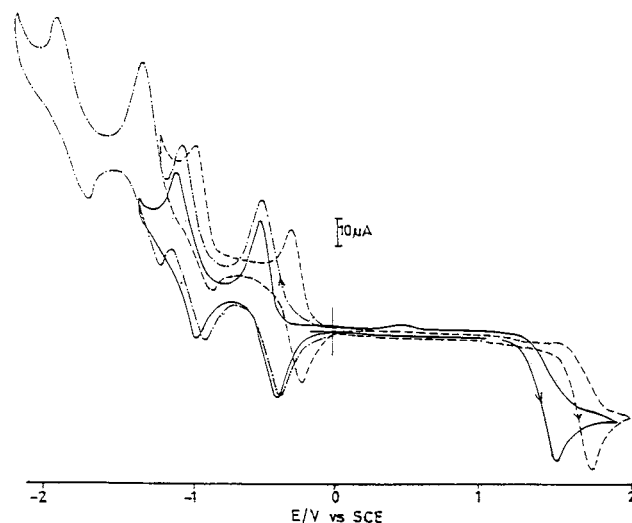

Fig. 3. Cyclic voltammograms (scan rate 50 mV s^{-1}) of a 10^{-3} mol dm^{-3} solution of [{NC$_5$H$_4$N=NC$_6$H$_4$(o-Me)}(CO)$_3$Re^0]$_2$ **1b** (–·–·–), [Re^I{NC$_5$H$_4$N=NC$_6$H$_4$(o-Me)}(CO)$_3$Cl] **2b** (—) and [Re^I{NC$_5$H$_4$N=NC$_6$H$_4$(o-Me)}(CO)$_3$ (CH$_3$CN)]ClO$_4$ **3** (-------) in acetonitrile at 298 K.

Table 4
Electrochemical data in acetonitrile solvent at 298 K^a

Compound	E_{pa} (V)^b	E_{298}° (V) (ΔE_p (mV))	
	Re^I–Re^{II}	Ligand reductions	
1a	–	–0.45 (90), –0.95(110), –1.21(100), –1.65(120)	
1b	–	–0.48(100), –1.01(110), –1.27(120), –1.73(120)	
1c	–	–0.41(90), –0.89(110), –1.19(120), –1.62(110)	
1d	–	–0.50(90), –1.04(100), –1.31(130), –1.77(100)	
1e	–	–0.38(80), –0.84(120), –1.15(120), –1.59(120)	
2a	1.54	–0.39(60), –0.85(120)	
2b	1.52	–0.48(70), –1.06(120)	
2c	1.55	–0.37(70), –0.84(110)	
2d	1.51	–0.42(70), –0.90(110)	
2e	1.58	–0.28(70), –0.83(120)	
3	1.78	–0.29(60), –0.91(130)	

^{a} Conditions: solvent, acetonitrile; supporting electrolyte, NBu$_4$ClO$_4$ (0.1 M); reference electrode, SCE; solute concentration, 10^{-3}M; working electrode, platinum; scan rate, 100 mV s^{-1}; $E_{298}^{\circ} = 0.5(E_{pc} + E_{pa})$ where E_{pc} and E_{pa} are the cathodic and anodic peak potentials, respectively.
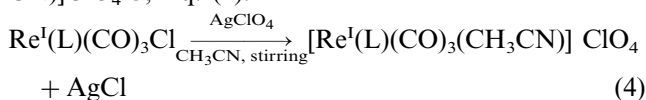
^{b} E_{pa} values are considered due to irreversible nature of the voltammograms.

unstable even at 258 K and this has precluded its further characterization. The one-electron nature of the second reduction process (Eq. (3)) is confirmed from the current height considerations. The formal potentials of the couples (Eqs. (2) and (3)) vary systematically depending on the nature of the substituents present on the ligand (Table 4).

The complexes 1 display four successive quasi-reversible ligand reductions (Fig. 3; Table 4) due to the presence of two ligands (L) in the complex.
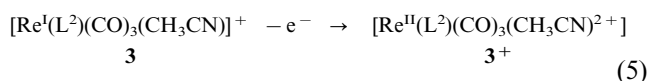
2.5. Chloride exchange reaction

In acetonitrile solvent the complexes 2 are susceptible to a chloride exchange in the presence of AgClO$_4$ at room temperature which results in an orange-colored acetonitrile complex of the type [Re^I(L)(CO)$_3$(CH$_3$CN)]ClO$_4$ 3, Eq. (4):

$$Re^I(L)(CO)_3Cl \xrightarrow[\text{CH}_3\text{CN, stirring}]{\text{AgClO}_4} [Re^I(L)(CO)_3(CH_3CN)]\ ClO_4$$
$$+ \ AgCl \qquad\qquad (4)$$

Here the exchange of a monoanionic chloride ligand by the neutral acetonitrile group takes place without any change in metal oxidation state or spin state. Although all the complexes (2a–2e) react similarly with AgClO$_4$ in presence of acetonitrile solvent and affording the species 3 readily, only the complex 2b has been isolated in pure solid state.

The diamagnetic complex 3 exhibits 1:1 conductivity in acetonitrile solution (Λ_M, 145 Ω^{-1} cm^2 mol^{-1}). The IR spectrum of 3 shows three CO stretching frequencies (Table 1) similar to the parent complex 2b (Fig. 2(c)) which supports the stereoretentive substitution reaction. A strong and broad vibration at 1097 cm^{-1} and a strong and sharp band at 624 cm^{-1} are observed due to the presence of ionic perchlorate. It exhibits MLCT transitions at 447 and 404 nm and a ligand based transition at 336 nm (Table 1). The complex 3 displays an irreversible Re$^I \rightarrow$ Re^{II} oxidation process (anodic peak, E_{pa}) at 1.78 V versus SCE (Eq. (5); Fig. 3).

$$[Re^I(L^2)(CO)_3(CH_3CN)]^+ \ -e^- \ \rightarrow \ [Re^{II}(L^2)(CO)_3(CH_3CN)^{2+}]$$
$$\mathbf{3} \qquad\qquad\qquad\qquad \mathbf{3^+} \qquad (5)$$

Under identical experimental conditions the E_{pa} of the Re$^I \rightarrow$ Re^{II} process of the corresponding chloro complex Re(L^2)(CO)$_3$Cl, 2b appears at 1.52 V. The observed 0.26 V positive shift of the rhenium(I)–rhenium(II) oxidation potential on moving from complex 2b to 3 reveals that the acetonitrile complex has superior redox stability for rhenium(I) as compared to the chloro-complex. It exhibits two quasi-reversible reductions at –0.29 and –0.91 V versus SCE (Fig. 3) due to successive two reductions of the azo group of coordinated ligand L^2.

The acetonitrile group of complex 3 can be replaced readily further by other monodentate ligands keeping the overall geometry of the complex intact.

The mechanism along with the general applicability of the silica gel mediated metal–metal bond cleavage reaction in other systems are under scrutiny.

3. Conclusion

Although the metal–metal bond of dirhenium carbonyl species, Re$_2$(CO)$_{10}$ and its derivatives are susceptible to photolytic Re–Re bond cleavage reaction, the interaction of arylazopyridine ligand (L) with the Re$_2$(CO)$_{10}$ results in stable metal–metal bonded complexes of the type (CO)$_3$LRe^0–Re^{0}L(CO)$_3$ 1 via the partial replacement of CO group from each of the rhenium centers of Re$_2$(CO)$_{10}$. However, on the silica gel column and in presence of chlorinated solvent (CHCl$_3$ or CH$_2$Cl$_2$) the nonphotolytic cleavage of the Re–Re bond of 1 and the oxidative chlorine addition to the rhenium center have taken place consecutively, affording a monomeric complex of the type Re^I(L)(CO)$_3$Cl 2. The effect of the presence of strong π-acidic ligands (L and CO) in the coordination environment of 2 have been reflected in the high metal oxidation potentials. The chloride group of 2 is susceptible to facile chloride exchange reaction.

4. Experimental

$Re_2(CO)_{10}$ was obtained from Aldrich, USA. The ligands L^1–L^5 were prepared by condensing 2-aminopyridine with the appropriate nitrosobenzene according to the reported procedure [14]. For spectroscopic and electrochemical studies HPLC grade solvents were used. Silica gel (60–120 mesh) used for chromatography was of BDH quality. Commercial tetrabutyl ammonium bromide was converted into pure tetrabutyl ammonium perchlorate by following an available procedure [18].

UV–visible spectra were recorded by using a Shimadzu-160 spectrophotometer. FT-IR spectra were taken on a Nicolet spectrophotometer with samples prepared as KBr pellets. Laser Raman spectra were taken in $CHCl_3$ using an Ar-ion laser system, Coherent, USA, attached to a Jobin Yvon Romonor HG2S spectrometer, France. Solution electrical conductivity was checked using a Systronic 305 conductivity bridge. Magnetic susceptibility was checked with a PAR vibrating sample magnetometer. NMR spectra were obtained with a 300 MHz Varian Fourier transform spectrometer. Cyclic voltammetric measurements were carried out using a PAR model 362 scanning-potentiostat electrochemistry system. Platinum wire working and auxiliary electrodes and an aqueous saturated calomel reference electrode (SCE) were used in a three electrode configuration. The supporting electrolyte was $[NBu_4]ClO_4$ and the solute concentration was $\sim 10^{-3}$ M. The half-wave potential E^0_{298} was set equal to 0.5 $(E_{pa} + E_{pc})$, where E_{pa} and E_{pc} are anodic and cathodic cyclic voltammetric peak potentials, respectively. Coulometric experiments were done with a PAR model 370-4 electrochemistry apparatus incorporating a 179 digital coulometer. A platinum wire-gauze electrode was used. All experiments were carried out under a dinitrogen atmosphere and were uncorrected for junction potentials. The FAB mass spectra at 298 K were recorded on a JEOL SX 102/DA-6000 mass spectrometer. The elemental analyses were carried out with Carlo Erba (Italy) elemental analyzer. Optical rotation was checked by using JASCO DIP-370 digital polarimeter. The EPR measurements were made with a Varian model 109C E-line X-band spectrometer fitted with a quartz Dewar for measurements at 77 K (liquid nitrogen). The spectra were calibrated by using tetracyanoethylene (TCNE) ($g = 2.0037$).

4.1. Synthesis

The syntheses of the complexes (**1** and **2**) were carried out using the following general procedures. Yields varied in the ranges 70–75%. and 65–70% for **1** and **2,** respectively. Details are given for one representative case.

4.1.1. Hexacarbonyl bis-(2-phenylazopyridine)-dirhenium(0),{$(L^1)(CO)_3Re^0$}$_2$ (1a) and tricarbonyl(chloro)(2-phenylazopyridine)rhenium(I), $Re^I(L^1)(CO)_3(Cl)$ (2a)

$Re_2(CO)_{10}$ (100 mg, 0.153 mmol) was dissolved in 15 ml of freshly distilled tetrahydrofuran (THF) under N_2 atmosphere. To this solution 2-phenylazopyridine ligand L^1 (75 mg, 0.41 mmol) in 5 ml of freshly distilled dry THF was added. The resulting mixture was heated to reflux for 3 h under a dinitrogen atmosphere. The initial red color of L^1 gradually changed to a red–brown color. The solvent was then removed under reduced pressure. The solid red–brown product thus obtained was washed thoroughly with hexane to remove the excess ligand and finally recrystallization from 1:1 acetonitrile–benzene yielded the complex **1a**. Yield 73%.

The complex **1a** dissolved in minimum volume of $CHCl_3$ and was subjected to chromatography on a silica gel (60–120 mesh) column. On elution with chloroform a deep pink colored band was separated leaving behind a dark band corresponding to the starting complex **1a** at the top of the column. The pink colored band was collected and evaporation of the solvent under reduced pressure afforded a crystalline solid product **2a**. The dark brown band was then eluted by acetonitrile. The repetition of similar chromatographic operation on the unaltered complex **1a** (recovered from the previous column) resulted in a second batch of complex **2a** in presence of $CHCl_3$ as eluent. Four similar chromatographic cycles were required for the complete transformation of **1a** to **2a**. Finally the product was recrystallized from dichloromethane-hexane (1:4). Yield 67%.

4.1.2. Tricarbonyl (acetonitrile){2-(ortho tolylazo)pyridine} rhenium(I) perchlorate [$Re^I(L^2)(CO)_3(CH_3CN)$]-ClO_4 (3)

$Re(L^2)(CO)_3Cl$, **2b** (100 mg, 0.199 mmol) was dissolved in 10 ml of acetonitrile. To this solution $AgClO_4$ (95 mg, 0.46 mmol) was added with stirring. The initial pink color of **2b** immediately changed to orange. The stirring was continued for 2 h. The solution was then filtered to remove AgCl precipitate and the solvent was removed from the filtrate under reduced pressure. The solid mass was then washed several times with ice-cold water to remove excess $AgClO_4$. The solid product was dried in vacuo over P_4O_{10}. Yield: quantitative.

4.2. Crystallography

Single crystals of complex **2a** were grown by slow diffusion of a dichloromethane solution of it in hexane. A dark cubic crystal of dimension $0.1 \times 0.1 \times 0.1$ mm^3 was selected for X-ray data collection. All measurements were made on a Rigaku AFC7S diffractometer

with graphite monochromated Cu–K_α radiation. The data were collected at a temperature of 293K using the ω–2θ scan technique. Cell constants and an orientation matrix for the data collected were determined from a least-squares refinement in the range $29.50 < 2\theta < 37.01°$ which corresponded to a primitive monoclinic cell with dimensions $a = 12.410(4)$ Å, $b = 9.080(2)$ Å, $c = 13.804(6)$ Å, $\beta = 102.60(3)°$, $V = 1518.0(9)$ Å^3, $Z = 4$, $\rho_{cald} = 2.139$ g cm^{-3}, $F_{000} = 920$, space group $P2_1$. Significant crystal data and data collection parameters are listed in Table 5.

An empirical absorption correction based on azimuthal scans [19] of several reflections was applied which resulted in transmission factors ranging from 0.106 to 1.00. A total of 1776 data were collected in the range of $3.28 \leq 2\theta \leq 49.97°$ of which 1681 were unique ($R_{int} = 0.05$). The structure was solved by direct method (SHELX-97) [20] and expanded using Fourier techniques. The function minimized throughout refinement was $\Sigma w(|F_o| - |F_c|)^2$ with $w = 1/\sigma^2(F_o)$. Final refinement wascarried out with anisotropic thermal parameter for all non-hydrogen atoms. Hydrogen atoms were included at the chemical positions and were not refined. The final cycle of full-matrix refinement (SHELX-97) was based on 1681 observed reflections ($I > 2\sigma(I)$) and 398 variable parameters. The refinement converged to $R_1 = 0.083$, $wR_2 = 0.2117$ and goodness of fit = 2.176. Atomic coordinates and isotropic thermal parameters are tabulated in Table 6.

5. Supplementary material

Crystallographic data for the structural analysis are available from the authors.

Table 5
Crystallographic data for **2a**

Chemical formula	$C_{28}H_{18}Cl_2N_6O_6Re_2$
f_w	977.78
Space group	$P2_1$
a (Å)	12.410(4)
b (Å)	9.080(2)
c (Å)	13.804(6)
β (°)	102.60(3)
V (Å^3)	1518(9)
Z	4
T (K)	293
λ (Å)	1.54178
ρ_{cald} (g cm^{-3})	2.139
μ (mm^{-1})	17.428
R_1	0.0831
wR_2	0.2117

Table 6
Atomic coordinates ($\times 10^4$) and equivalent isotropic displacement parameters (Å$^2 \times 10^3$) for **2a**[a]

	x	y	z	U_{eq}
Re(1)	0.48688(11)	0.44413(8)	0.73099(10)	0.0489(8)
Cl(1)	0.4109(6)	0.4155(15)	0.8796(6)	0.063(3)
C(1A)	0.733(2)	0.231(4)	0.822(2)	0.053(9)
C(2A)	0.823(2)	0.174(6)	0.873(2)	0.061(9)
C(3A)	0.828(2)	0.052(4)	0.921(2)	0.069(9)
C(4A)	0.726(2)	−0.030(5)	0.926(2)	0.062(9)
C(5A)	0.621(3)	0.027(5)	0.863(2)	0.063(8)
C(6A)	0.620(3)	0.143(4)	0.817(3)	0.044(10)
N(7A)	0.5270(19)	0.218(5)	0.7550(17)	0.046(7)
N(8A)	0.446(3)	0.131(5)	0.721(2)	0.062(8)
C(9A)	0.351(3)	0.173(6)	0.672(2)	0.052(8)
C(10A)	0.275(2)	0.086(4)	0.628(2)	0.048(7)
C(11A)	0.171(3)	0.137(3)	0.570(3)	0.038(7)
C(12A)	0.157(2)	0.286(4)	0.570(2)	0.039(7)
C(13A)	0.242(2)	0.377(4)	0.610(2)	0.048(7)
N(14A)	0.346(3)	0.318(5)	0.658(2)	0.070(8)
C(15A)	0.543(3)	0.463(6)	0.618(2)	0.084(12)
O(16A)	0.5781(18)	0.477(4)	0.5470(17)	0.090(11)
C(17A)	0.615(3)	0.546(3)	0.794(3)	0.058(9)
O(18A)	0.691(2)	0.614(5)	0.847(2)	0.090(9)
C(19A)	0.433(6)	0.631(7)	0.716(4)	0.100(18)
O(20A)	0.387(3)	0.756(4)	0.670(3)	0.093(11)
Re(2)	0.98692(10)	0.18805(8)	0.23042(10)	0.0498(8)
Cl(2)	0.9090(6)	0.2130(19)	0.3819(5)	0.069(3)
C(1B)	1.132(3)	0.611(4)	0.374(2)	0.060(8)
C(2B)	1.221(2)	0.665(5)	0.426(2)	0.060(8)
C(3B)	1.313(3)	0.602(5)	0.4281(19)	0.061(8)
C(4B)	1.318(3)	0.465(6)	0.368(3)	0.067(9)
C(5B)	1.216(3)	0.408(5)	0.317(3)	0.069(10)
C(6B)	1.132(3)	0.470(4)	0.315(2)	0.040(7)
N(7B)	1.025(2)	0.423(5)	0.2545(19)	0.051(8)
N(8B)	0.964(3)	0.523(4)	0.228(4)	0.049(8)
C(9B)	0.855(3)	0.463(6)	0.166(3)	0.054(9)
C(10B)	0.765(3)	0.567(5)	0.133(3)	0.067(10)
C(11B)	0.674(4)	0.506(6)	0.093(3)	0.076(12)
C(12B)	0.661(4)	0.368(7)	0.065(4)	0.098(12)
C(13B)	0.754(3)	0.269(5)	0.112(3)	0.085(11)
N(14B)	0.8448(19)	0.314(3)	0.1641(19)	0.035(6)
C(15B)	1.0450(18)	0.184(6)	0.1136(18)	0.049(8)
O(16B)	1.0770(14)	0.187(4)	0.0411(14)	0.063(6)
C(17B)	1.114(2)	0.102(5)	0.309(2)	0.056(9)
O(18B)	1.190(2)	0.040(4)	0.349(2)	0.087(9)
C(19B)	0.924(3)	−0.007(5)	0.192(4)	0.050(11)
O(20B)	0.893(4)	−0.117(4)	0.197(4)	0.114(15)

[a] U_{eq} is defined as one third of the trace of the orthogonalized U_{ij} tensor.

References

[1] (a) J.M. O'Connor, in: E.W. Abel, F.G.A. Stone, G. Wilkinson and C.D. Casey (Eds.), Comprehensive Organometallic Chemistry, vol. 6, Pergamon, Press, New York, 1995, p. 167. (b) C.C. Romao, in: R.B. King (Ed.), Encyclopedia of Inorganic Chemistry, vol. 6, Wiley, NY, 1994, p. 3437. (c) D.B. MacQueen, K.S. Schanze, J. Am. Chem. Soc. 113 (1991) 7470. (d) P.O. Nubel, T.L. Brown, J. Am. Chem. Soc. 106 (1984) 644. (e) D.L. Morse, M.S.Wrighton, J. Am. Chem. Soc. 98 (1976) 3931. (f) K.S. Schanze, D.B. MacQueen, T.A. Perkins, L.A. Cabana, Coord. Chem. Rev. 122 (1993) 63.

[2] A.M. Stolzenberg, E.L. Mutterties, J. Am. Chem. Soc. 105 (1983) 822.

[3] A. Seal, S. Ray, Acta Crystallogr. Sect. C 40 (1984) 929.

[4] B.K. Ghosh, A. Mukhopadhyay, S. Goswami, S. Ray, A. Chakravorty, Inorg. Chem. 23 (1984) 4633.

[5] G.K. Lahiri, S. Goswami, L.R. Falvello, A. Chakravorty, Inorg. Chem. 26 (1987) 3365.

[6] (a) B.R. Davis, J.A. Ibers, Inorg. Chem. 10 (1971) 578. (b) C.P. Hrung, M. Tsutsui, D.L. Cullen, E.F. Meyer Jr, C.N. Morimoto, J. Am. Chem. Soc. 100 (1978) 6068.

[7] B.K. Santra, G.A. Thakur, P. Ghosh, A. Pramanik, G.K. Lahiri, Inorg. Chem. 35 (1996) 3050.

[8] B.K. Santra, G.K. Lahiri, J. Chem. Soc. Dalton Trans. (1997) 129.

[9] (a) T.G. Spiro, Prog. Inorg. Chem. 11 (1970) 1. (b) J. Lewis, A.R. Manning, J.R. Miller, M.J. Ware, F. Nyman, Nature 207 (1965) 142.

[10] M.S. Wrighton, D.L. Morse, J. Am. Chem. Soc. 96 (1974) 988.

[11] N. Bag, A. Pramanik, G.K. Lahiri, A. Chakravorty, Inorg. Chem. 31 (1992) 40.

[12] B.K. Ghosh, S. Goswami, A. Chakravorty, Inorg. Chem. 22 (1983) 3358.

[13] B.K. Santra, G.K. Lahiri, J. Chem. Soc. Dalton Trans. (1997) 1883.

[14] B.K. Santra, G.K. Lahiri, J. Chem. Soc. Dalton Trans. (1998) 139.

[15] A. Pramanik, N. Bag, D. Ray, G.K. Lahiri, A. Chakravorty, Inorg. Chem. 30 (1991) 410. (b) H. Taube, Pure Appl. Chem. 51 (1979) 901. (c) M. Sekine, W.D. Harman, H. Taube, Inorg. Chem. 27 (1988) 3604.

[16] S. Goswami, A.R. Chakravarty, A. Chakravorty, Inorg. Chem. 20 (1981) 2246.

[17] R.S. Drago, Physical methods for chemists, Saunders College Publishing, NY, 1992, p. 590.

[18] D.T. Sawyer, A. Sobkowiak, J.L. Roberts Jr, Experimental electrochemistry for chemists, Wiley, NY, 1995.

[19] A.C.T. North, D.C. Philips, F.S. Mathews, Acta Crystallogr. Sect. A 24 (1968) 351.

[20] G.M. Sheldrick, SHELXTL 97, Crystal structure refinement program, University of Gottingen, Germany, 1997.